

双二茂铁 - 钯配合物的合成, 结构和电化学

陈 光 区升举 白志平* 韩 刚 段春迎*

(南京大学配位化学研究所, 配位化学国家重点实验室, 南京 210093)

本文讨论了由二茂铁的 C-H... π 作用组装的具有类环己烷结构的氨基硫脲钯金属配合物的结构和电化学性能。晶体结构中钯原子以顺式平面正方形的构型分别与两个氨基硫脲配体配位, 两个配体中的二茂铁基团位于钯原子同一侧, 每个二茂铁与相邻分子中的二茂铁基团通过环戊二烯基环间的 C-H... π 作用形成由类环己烷结构连通的二维网状结构。对钯的配合物及相关的镍和锌配合物的电化学研究表明, 平面正方形的钯和镍可以有有效的传递两个茂铁间的氧化-还原性能。

关键词: 二茂铁 顺式构造 自组装 C-H... π 作用 电化学
分类号: O611.4 O614.81*1 O614.82*3

Synthesis, Crystal Structure and Electrochemistry of Biferrocene Palladium Complex

CHEN Guang OU Sheng-Ju BAI Zhi-Ping* HAN Gang DUAN Chun-Ying*

(Coordination Chemistry Institute, State Key Laboratory of Coordination Chemistry, Nanjing University, Nanjing 210093)

A new supramolecular cyclohexane-like structure $[\text{PdL}_2]_6$ (HL = acetylferrocenyl thiosemicarbazone) has been constructed by self-assembly of ferrocene moieties via C-H... π interactions. The palladium (II) atom is coordinated in a distorted square-planar cis-configuration in which two ferrocene-containing ligands positioned on the same side. Each ferrocene moieties interacts with symmetry-related species to form a two dimensions supramolecular network. Electrochemical measurements of $[\text{PdL}_2]$, $[\text{NiL}_2]$ and $[\text{ZnL}_2]$ compounds indicate that the square planar configuration of the Ni (II) and Pd (II) moieties, can effectively transmit the redox effects of the ferrocene moieties. CCDC: 157536.

Keywords: ferrocene, cis-configuration self-assembly C-H... π interaction electrochemistry

0 Introduction

Interactions between aromatic molecules present an important class of intermolecular force in chemistry, biology, materials science and crystallography^[1,2]. It is generally recognized that^[3], in the absence of strong hydrogen-bond donor and acceptors, aromatic compounds trend to self-assemble via π - π (face-face) interactions, C-H... π interactions (T-shape geome-

try, edge-face or herringbone interactions), and these weak non-covalent bonds can sustain supramolecular synthons which are structure determining^[4,5]. In our previous work, we introduced the ferrocene moieties in the nickel (II) and the zinc (II) compounds, the powder X-ray diffraction analyses of the palladium (II) complex and other metal complexes clearly indicate that cyclohexane aggregation between the ferrocene moieties is robust enough to be transformed from one structure to

收稿日期:2003-01-20。收修改稿日期:2003-04-04。

国家自然科学基金资助项目(No. 20131020)。

* 通讯联系人。E-mail: baizp@nju.edu.cn; duancy@nju.edu.cn

第一作者:陈 光,男,24岁,硕士研究生;研究方向:功能配位化学。

another^[6]. To test this approach, here we report the crystal structure and electrochemistry study on the palladium complex.

On the other hand, bridged biferrocenes have been proven to be good candidates for mixed-valence compounds owing to their variability in structure and suitability for study with several physical techniques^[7, 8]. It is postulated that if the ferrocene moieties are bridged by a square planar configuration d^8 metal compound^[9], redox effects of the ferrocene moieties should be transmitted. To further study the electron transfer between the ferrocene moieties of metal-bridged biferrocene compounds, electrochemistry of the title compound and relative compounds are reported.

1 Experimental Detail

1.1 General Comments

Thiosemicarbazide and acetylferrocene (Aldrich) were used as received. The ligand, acetylferrocenyl thiosemicarbazone, the nickel and zinc complexes are prepared according to the literature^[6]. All other chemicals were of reagent grade quality obtained from commercial sources and used without further purification. Electronic absorption spectra were obtained on a Shimadzu UV-240 spectrophotometer in dichloromethane solution. Elemental analyses of carbon, nitrogen, and hydrogen were performed on a Perkin-Elmer 240 analytical instrument. Differential-pulse voltammetry measurement were done with an EG and GPAR model 273 instrument, which has a 50ms pulse width, with current sample 40 ms after the pulse was applied. A sweep rate of $25\text{mV} \cdot \text{s}^{-1}$ was used in all pulse experiments. The cell comprises of a platinum-wire-working electrode, a platinum auxiliary electrode and an Ag wire reference electrode. Current-potential curves were displayed on an IBM computer using model 270 electrochemical analysis software. The voltammograms of the complexes were obtained in dichloromethane with $n\text{-Bu}_4\text{NClO}_4$ ($0.1\text{mol} \cdot \text{L}^{-1}$) as the electrolyte and ferrocene ($2.0 \times 10^{-3}\text{mol} \cdot \text{L}^{-1}$) as internal standard.

Caution! Although no problems were encountered

in this work, the salt perchlorate are potentially explosive. They should be prepared in small quantities and handled with care.

1.2 Synthesis of the Palladium Complex

Ethanol solutions (25mL) of acetylferrocenyl thiosemicarbazone HL (0.42g, 1mmol) and $\text{Pd}(\text{CH}_3\text{CN})_2\text{Cl}_2$ (0.26g, 1mmol) were mixed. After refluxing for 4h, the dark brown solid formed was isolated, washed with ethanol and dried under vacuum. Yield 0.56g (73%) of the palladium complex. Anal. Found: C, 42.5; H, 3.4; N, 11.5. $\text{C}_{26}\text{H}_{30}\text{Fe}_2\text{N}_6\text{OPdS}_2$. Calc: C, 43.1; H, 4.2; N, 11.6%. The crystals of $[\text{PdL}_2]$ suitable for X-ray structural analyses were obtained by slow evaporation of the CHCl_3 solution in air.

1.3 X-ray Data Collection and Solution

Parameters for data collection and refinement of the title complex are summarized in Table 1. Intensities were collected on a Siemens SMART-CCD diffractometer with graphite-monochromatic $\text{MoK}\alpha$ radiation ($\lambda = 0.071073\text{nm}$) using SMART and SAINT^[10] program. The structure was solved by direct methods and refined on F^2 using full-matrix least-squares methods using SHELXTL version 5.1^[11]. Anisotropic thermal parameters were refined for non-hydrogen atoms. Hydrogen atoms were localized in their calculation positions and refined using riding model.

CCDC: 157536.

Table 1 Crystallographic Data for Complex $[\text{PdL}_2]$

formula	$\text{C}_{27}\text{H}_{34}\text{Fe}_2\text{N}_6\text{O}_2\text{PdS}_2$
<i>M</i>	756.82
<i>T</i> /K	293(2)
crystal system	trigonal
space group	$R\bar{3}$
<i>a</i> /nm	2.9925(4)
<i>c</i> /nm	1.8436(4)
<i>V</i> /nm ³	14.928(4)
<i>Z</i>	18
$\rho_{\text{calc}}/(\text{g} \cdot \text{cm}^{-3})$	1.582
μ/mm^{-1}	1.626
$R_1, wR_2 [I > 2\sigma(I)]$	0.061, 0.161

$$R_1 = \sum ||F_o| - |F_c|| / \sum |F_o|;$$

$$wR_2 = [\sum w(F_o^2 - F_c^2)^2 / \sum w(F_o^2)^2]^{1/2}.$$

2 Results and Discussion

2.1 Structure of Palladium Complex PdL₂

Fig. 1 shows an ORTEP plot of the palladium (II) complex **1** with atomic numbering scheme. The palladium atom is coordinated in a distorted square-planar *cis*-configuration with two ferrocene moieties positioned on the same side [N(3)-Pd(1)-N(6) 102.7(2), S(1)-Pd(1)-S(2) 94.2(1)] (Table 2). The mean deviation of the PdSSNN coordination plane is ca. 0.025 nm. The crowding between the two ligands in the complex is relieved by the molecule assuming a step conformation. The dihedral angles between the PdSSNN coordination plane and two SCNN planes are 22.5° on an average. It is suggested that the *cis*-configuration is stabilized by the stacking interactions between the acetylcyclopentadienyl rings. The dihedral angle of the stacked pair is 15°, the shortest inter-planar atom...atom separation is 0.346 nm. This distance is comparable with the standard distance for a

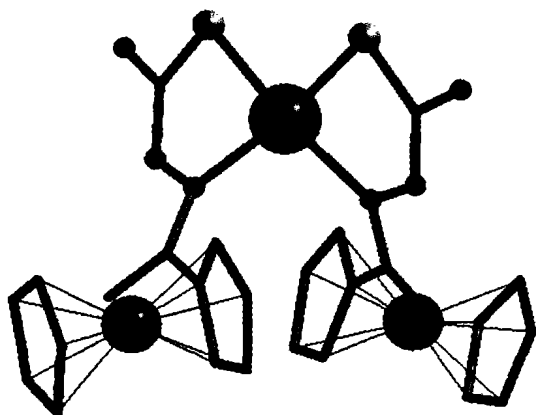


Fig. 1 Molecular structure of the title compound with the atom numbering scheme. Hydrogen atoms apart from those on water molecules are omitted for clarity

strong π -stacking interaction between two aryl rings (0.335 nm)^[12] in graphite and 0.310 nm for fluorene rings^[13].

The molecules connect with one another to form a cyclohexane-like hexamer via aromatic C-H... π interactions between ferrocene moieties (Fig. 2), like that of [NiL₂]. The cyclic hexamer comprises six symmetry-related Cp rings. Since the hexamer lies on a crystallographic S₃ axis, it adopts a chiral geometry. The shortest distance between the centroid of the Cp

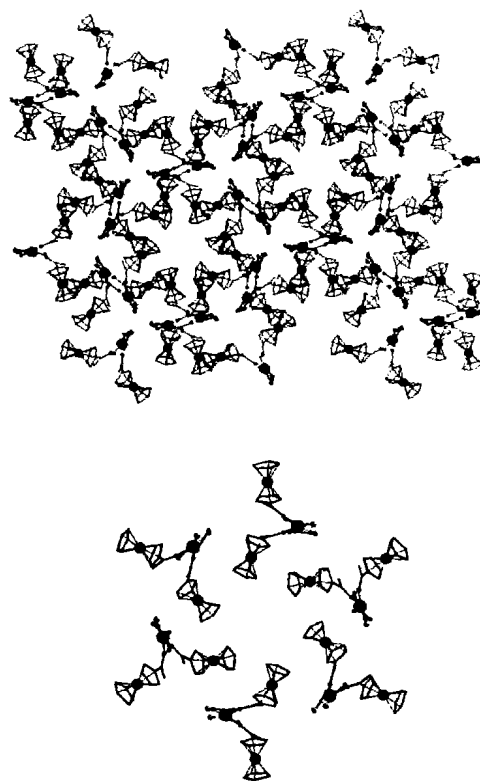


Fig. 2 Molecular packing of the cyclohexane-like network of the palladium (II) complex

The solvent molecules and the ethyl groups as well as the hydrogen atoms are omitted for clarity.

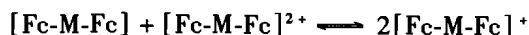
Table 2 Selected Bond Lengths ($\times 10^{-1}$ nm) and Angles ($^{\circ}$) for the Palladium Complex

Pd(1)-N(3)	2.046(4)	Pd(1)-N(6)	2.051(4)	Pd(1)-S(1)	2.236(1)	Pd(1)-S(2)	2.226(1)
S(1)-C(1)	1.750(5)	N(1)-C(1)	1.357(7)	N(2)-C(1)	1.294(7)	N(2)-N(3)	1.395(6)
N(3)-C(2)	1.313(6)	S(2)-C(14)	1.761(5)	N(4)-C(14)	1.344(6)	N(5)-C(14)	1.294(7)
N(5)-N(6)	1.403(5)	N(6)-C(15)	1.295(6)				
N(3)-Pd(1)-S(2)	169.3(1)	N(3)-Pd(1)-N(6)	102.7(2)	S(2)-Pd(1)-S(1)	94.2(1)	N(3)-Pd(1)-S(1)	83.3(1)
N(6)-Pd(1)-S(2)	81.8(1)	N(6)-Pd(1)-S(1)	168.0(1)				

ring [defined by C(9), C(10), C(11), C(12) and C(13)] in one molecule and the interacting C atom C(11) ($1 - x, 1 - x + y, 0.66667 - z$) in a symmetry-related molecule is 0.385nm (H...centroid 0.303nm, C-H...centroid 141), the inter-plane angle is 69° . It should be noted that this distance is a little longer than those found in the crystal structure of benzene (0.378nm and 85°)^[14] and similar to the honeycomb arrangement in the crystal structure of complexes of 1, 3, 5-trihydroxybenzene with 4-methylpyridines (0.385nm and 89°)^[3].

2.2 Electrochemistry

Differential pulse voltammetry (DPV) technique is usually employed to obtain well-resolved potential information, while the individual redox processes for the multi-nuclear complexes are poorly resolved in the CV experiment, in which individual $E_{1/2}$ potentials cannot be easily or accurately extracted from this data. Biferrocenes generally show two successive reversible one-electron oxidations $E_1(E_{[Fc_2]^{+2}/[Fc_2]})$ and $E_2(E_{[Fc_2]^{+3}/[Fc_2]^{+2}})$, separated by ΔE to yield the mono- and dications, respectively. The solution-state differential pulse voltammograms (Fig. 3a) of the title complex PdL₂, like those of other biferrocene complexes, show two peaks with half-wave potentials ($E_{1/2}$) at 0.70 and 0.91V, respectively. The ΔE values of ca. 0.21V indicate strong interactions between two ferrocene moieties in the corresponding complexes^[15]. The equilibrium constants K_{com} of the equation can be calculated by use of the Nernst equation from the ΔE as 3.6×10^3 .



(where Fc represents a ferrocenyl unit and M represents the bridging metal center). While related nickel compound NiL₂(Fig. 3b) also exhibits two sequential reversible one-electron oxidations with half-wave potentials ($E_{1/2}$) at 0.73V and 0.85V, respectively, the zinc complexes ZnL₂ exhibits only a single peak with half-wave potentials ($E_{1/2}$) at 0.79V. It has been postulated that a statistical contribution of 36mV holds for identical, non-interacting metal ions in the homobinuclear complexes, the small ΔE value (36mV) between two voltammetric waves always led to the two

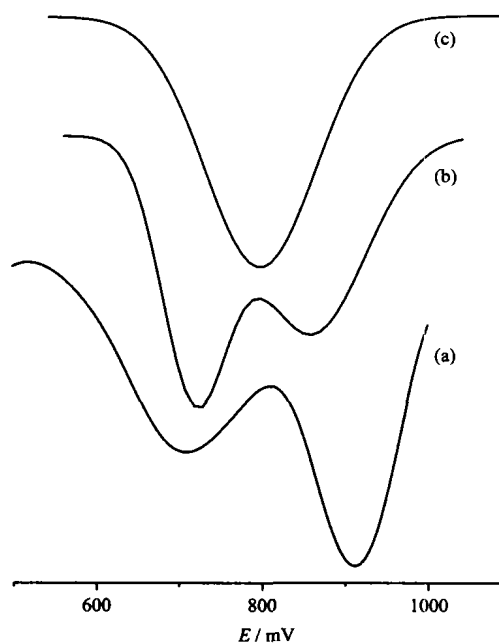


Fig. 3 Differential-pulse voltammetry of the complexes in CH₂Cl₂ containing *n*-Bu₄NClO₄(0.1 mol · L⁻¹); (a) PdL₂, (b) NiL₂, (c) ZnL₂ in CH₂Cl₂ solution containing *n*-Bu₄NClO₄(0.1 mol · L⁻¹) at a scanning rate of 20mV · s⁻¹(vs AG/AgCl)

waves coupled each other and only one broad peaks appeared in the DPV. In this case, the only one broad peak of the zinc complexes indicates that the two ferrocene moieties are identical and there is no interaction between them.

The ΔE with K_{com} depends on a number of factors^[16, 17]. (1) Major structural changes such as bond making and breaking, changes in coordination number, and severe changes in coordination geometry upon charge transfer can shift proportional equilibrium. (2) If the metal ions are in close proximity, a through space coulomb interaction may be important. (3) Electron delocalization in mixed oxidation states will enhance the stability of these species with resulting increases in ΔE . As suggested by our previously work, the trinuclear complexes were designed to help quantitatively define some of these effects. First, since crystallographic data on ferrocene^[18] and ferrocenium^[19] indicate the oxidation state and charge of the iron atom have almost no effect on the inter-atomic distances, it

is likely that only negligible structural changes accompany one-electron oxidation of the complexes. Second, through space metal-metal coulomb contribution to the Fc^+/Fc oxidation potential in Fc-M-Fc complexes are essentially constant and could be cancelable, since the distance between iron atoms are almost same for the three complexes, and are quite close to 0.76nm, the average encounter diameter between ferrocene and ferrocenium ion in solution. In fact, these metal-bridged biferrocene complexes designed here are used to minimize the through space iron-iron interaction between the ferrocene moieties. Third, the electrochemistry for these metal bridges complexes accounts for structural, Coulomb as explained above. The difference in electrochemistry of these complexes then can be described to the difference in stability associated with a degree of electronic delocalization in these complexes. In the nickel and palladium complexes, the squareplanar configuration of the metal center, the empty d_{z^2} orbital can allow the electron moving in the whole molecule freely, while in the zinc complex, the tetrahedral coordinated of the center complex can not stabilized can minimize the electron transfer in the whole molecule.

References

- [1] (a) Hunter C. A. *Chem. Soc. Rev.*, **1994**, 101;
 (b) Hunter C. A. *J. Mol. Biol.*, **1993**, **230**, 1025;
 (c) Hunter C. A. *J. Am. Chem. Soc.*, **1992**, **114**, 5003.
- [2] (a) Desiraju G. R. *Angew. Chem., Int. Ed. Engl.*, **1995**, **34**, 2311;
 (b) Desiraju G. R. *Chem. Commun.*, **1997**, 1475.
- [3] (a) Biradha K., Zaworotko M. J. *J. Am. Chem. Soc., Chem. Commun.*, **1989**, 621;
 (b) Zorky P. M., Zrukya O. N. *Adv. Mol. Struct. Res.*, **1993**, **3**, 147.
- [4] (a) Houk K. N., Menzer S., Newon S. P., Raymo F. M., Stoddart J. F., Williams D. J. *J. Am. Chem. Soc.*, **1999**, **121**, 1479;
 (b) Paliwal S., Gerb S. L., Wilcox C. S. *J. Am. Chem. Soc.*, **1994**, **116**, 4497
- [5] Dance I., Scudder M. *J. Chem. Soc., Dalton Trans.*, **1998**, 1341; *Ibid.*, **1996**, 3755.
- [6] Fan C. J., Duan C. Y., He C., Han G., Meng Q. J. *New J. Chem.*, **2000**, **24**, 697.
- [7] Hendrickson D. N., Oh S. M., Dong T. Y., Kambara T., Cohn M. J., Moore M. F. *Inorg. Chem.*, **1985**, **4**, 329.
- [8] Webb R. J., Dong T. Y., Pierpont C. G., Bonne S. R., Chadha R. K., Hendrickson D. N. *J. Am. Chem. Soc.*, **1991**, **113**, 4806.
- [9] Duan C. Y., Tian Y. P., Liu Z. H., You X. Z., Mak C. W. Thomas *J. Organometallic Chem.*, **1998**, **570**, 155.
- [10] SMART and SAINT, Area Detector Control and Integration Software, Siemens Analytical X-Ray Systems, Inc., Madison, Wisconsin, USA, **1996**.
- [11] Sheldrick G. M. *SHELXTL V5.1 Software Reference Manual*, Bruker AXS, Inc., Madison, Wisconsin, USA, **1997**.
- [12] Shriver D. F., Arkins P., Langford C. H. *Inorg. Chem. 2nd edn.*, Freeman W. H. and Company: New York, **1997**.
- [13] Liu Z. H., Duan C. Y., Hu J., You X. Z. *Inorg. Chem.*, **1999**, **38**, 1719.
- [14] Bacon G. E., Curry N. A., Wilson S. A. *Proc. R. Soc. London, Ser. A*, **1964**, **279**, 98.
- [15] Creutz C., Taube H. *J. Am. Chem. Soc.*, **1973**, **95**, 1086.
- [16] Tom G. M., Creutz C., Taube H. *J. Am. Chem. Soc.*, **1974**, **96**, 7828.
- [17] Weaver T. R., Mayer T. J., Adeylmi S. A., Brwon G. M., Eckberg R. P., Hatifield E., Johnson E. C., Murray R. W., Unterker D. *J. Am. Chem. Soc.*, **1975**, **97**, 3039.
- [18] Rosenblum *Chemistry of the Iron Group Metallocenes*, New York, **1965**.
- [19] Bernstein T., Herbstein F. H. *Acta Crystallogr. Sect. B*, **1968**, **24**, 1546.